

## Small-Angle Neutron Scattering Analysis of Blends with Very Strong Intermolecular Interactions: Polyamide/Ionomer Blends

R. T. Tucker,<sup>†,‡,#</sup> C. C. Han,<sup>‡,&</sup> A. V. Dobrynin,<sup>‡,§</sup> and R. A. Weiss<sup>\*,†,‡</sup>

Department of Chemical Engineering, Polymer Program, and Department of Physics, University of Connecticut, Institute of Materials Science, 97 N. Eagleville Rd., Storrs, Connecticut 06269-3136, and Polymers Division, National Institute of Standards and Technology, Gaithersburg, Maryland 20899

Received February 14, 2003; Revised Manuscript Received April 16, 2003

**ABSTRACT:** Partially miscible blends of the lithium salt of sulfonated polystyrene ionomer (Li-SPS) and a methylated polyamide (mPA) were studied using small-angle neutron scattering. The blends exhibit lower critical solution temperature behavior (LCST), and the LCST increases with increasing sulfonation level of the ionomer. When the sulfonation level of the ionomer was below 20 mol %, a peak was observed in the scattering structure factor. The position of the peak moved to lower wavevector with increasing sulfonation level and with increasing temperature. The origin of the peak was a correlation hole due to the essential formation of a graft copolymer by the formation of an ion–dipole complex between the amide and sulfonate groups. The tendency of the unsulfonated polystyrene to phase separate from the polyamide was suppressed by the complexation, but it also produced large concentration fluctuations in the blends. The size and intensity of the concentration fluctuations increased with increasing temperature, i.e., as the LCST phase boundary was approached, and decreased with increasing sulfonation level as the length of the unsulfonated chain between sulfonate groups (and complex sites) decreased. The SANS data were successfully modeled with a modified form of the de Gennes model for scattering from a cross-linked polymer blend, which allowed for calculation of an interaction parameter,  $\chi$ , for the system. In general,  $\chi$  decreased with increasing sulfonation level and with increasing ionomer composition.

### Introduction

Polymer blends are most often immiscible due to the small combinatorial entropy of mixing for high molecular weight compounds. Miscibility can be achieved by promoting intermolecular exothermic interactions such as hydrogen bonding,<sup>1–5</sup> ion–dipole interactions,<sup>6</sup> acid–base interactions,<sup>7</sup> and transition metal complexation.<sup>8</sup> An increasingly popular strategy for enhancing the miscibility of two polymers is to attach ionic groups to one polymer that form specific attractive interactions with a complementary functional group on the second polymer. For example, lightly sulfonated polystyrene ionomers (SPS) mix with polyamides<sup>9–22</sup> as a result of strong ion–dipole interactions between the metal sulfonate and amide groups.

We previously reported on the nature of the specific interactions and the phase behavior determined by light scattering of blends of SPS ionomers and an N,N'-methylated nylon 2-12 (mPA).<sup>20–22</sup> The use of the mPA inhibited hydrogen-bonding interactions within the polyamide and between the two polymers, which provided an unambiguous characterization of the effect of ion–dipole interactions on the thermodynamics and properties of the blends. The absence of hydrogen bonding also provided a low melting point (~70 °C), which allowed us to access the polyamide melt at relatively low temperatures and, therefore, suppress

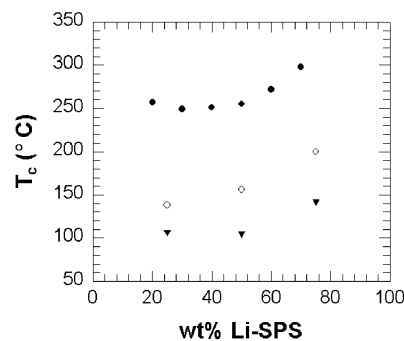


**Figure 1.** Cloud point curves determined by light scattering for LiSdPS/mPA blends for various sulfonation levels: (▼) 4.0, (○) 5.2, and (●) 9.5 mol %.

degradation. In addition, the crystallization kinetics of the polyamide were slow, so that it was fairly easy to prepare amorphous blends.

Ion–dipole complexation between the metal cation of SPS and the carbonyl oxygen of the amide groups in the mPA produced physical cross-links that promoted miscibility.<sup>20</sup> The blends exhibited lower critical solution temperature (LCST) phase behavior (see Figure 1), the temperature of which was sensitive to the sulfonation level for the ionomer and the choice of cation.<sup>22</sup> The ion–dipole cross-links are in equilibrium with nonassociated metal sulfonate and amide groups, and the relative number of associations is temperature-dependent. At low temperature, the equilibrium favors the sulfonate–amide complex, which is responsible for the miscibility of the blend. As temperature increases, however, the equilibrium shifts toward the nonassociated species, and the number of intermolecular cross-links eventually falls below a critical value needed to maintain a miscible blend. For a fixed blend composition, increasing the sulfonation level of the ionomer increases the LCST by

<sup>†</sup> Department of Chemical Engineering, University of Connecticut.

<sup>‡</sup> Polymer Program, University of Connecticut.

<sup>§</sup> Department of Physics, University of Connecticut.

<sup>‡</sup> National Institute of Standards and Technology.

<sup>#</sup> Current address: Specialized Technology Resources, Inc., 10 Water St., Enfield, CT 06082-4899.

<sup>\*</sup> Current address: Joint Laboratory of Polymer Science and Materials, Institute of Chemistry, The Chinese Academy of Sciences, Zongguancun, Beijing, China 100080.

**Table 1. Polymer Samples**

sample	$M_w^a$	$M_w/M_n^a$	$T_g, ^\circ\text{C}$
5.7% LiSdPS	107 000	1.07	118
8.7% LiSdPS	107 000	1.07	118
11.3% LiSdPS	107 000	1.07	120
20% LiSdPS	107 000	1.07	126
mPA	65 000	2.6	0

<sup>a</sup> Molecular weight averages measured on parent polystyrenes.

effectively increasing the number of virtual cross-linking sites at all temperatures. The interactions with the polyamide also suppress microphase separation of the ionomer in the blend.

The SPS/mPA blends exhibit anomalous phase separation behavior<sup>22</sup> in that conventional spinodal decomposition kinetics are not followed. Instead of the growth of a dominant wavelength in the light scattering data, a broad range of size scales grow simultaneously during phase separation, and the phase separation process stalls and the structure is "pinned" after a relatively short time. The structure pinning is due to the microphase separation of ionic aggregates in the ionomer-rich phase during phase separation.

The purpose of the investigation reported herein was to further characterize the phase behavior and microstructure of the SPS/mPA blends using small-angle neutron scattering (SANS).

### Experimental Details

**Materials.** Sulfonated perdeuterated polystyrene, SdPS, was prepared by solution sulfonation of perdeuterated ( $d_8$ ) polystyrene ( $M_w = 107\,000$  g/mol;  $M_w/M_n = 1.07$ ) with acetyl sulfate following the procedure of Makowski et al.<sup>23</sup> This sulfonation process attaches sulfonic acid groups randomly along the polystyrene chain and primarily at the para position of the phenyl ring. The sulfonation level was determined by titration of the sulfonic acid derivative, HSdPS, in a mixed solvent of toluene/methanol (90/10 v/v) with methanolic sodium hydroxide. Four different HSdPS samples were prepared with sulfonation levels of 5.7, 8.7, 11.3, and 20 mol %, where mol % denotes the percentage of styrene groups that were sulfonated. The HSdPS samples were converted to lithium salts (LiSdPS) by neutralization with a stoichiometric amount of lithium hydroxide. The nomenclature used hereafter for the ionomers is  $x.y$ LiSdPS, where  $x.y$  denotes the sulfonation level in mol %.

Poly( $N,N$ -dimethylethylene sebacamide), mPA, was synthesized following the procedure of Huang et al.<sup>24</sup> Gel permeation chromatography (GPC) and differential scanning calorimetry (DSC) were used to measure the molecular weight averages and glass transition temperatures of the starting polymers (see Table 1).

Blends with various compositions were prepared by adding a 3% (w/v) mPA solution in 1,2-dichloroethane/methanol (90/10 v/v) dropwise to a stirred 3% solution of LiSdPS in 1,2-dichloroethane/methanol (90/10 v/v). Blend samples for SANS were cast from solution into a poly(tetrafluoroethylene) dish, dried in a vacuum oven at 80 °C for 2 days, and then melt-pressed into 1 mm thick disks. Prior to the SANS experiments, all samples were annealed at 120 °C for 15 h. All samples were optically transparent.

Small-angle neutron scattering (SANS) experiments were carried out on the 30 m instrument at the Cold Neutron Research Facility of the National Institute of Standards and Technology (Gaithersburg, MD). A velocity selector was used to monochromatize the incident beam wavelength,  $\lambda$ , to 0.6 nm. The neutron detector was a 2D position-sensitive, ILL-type area detector that moved along rails inside a vacuum-enclosed, cylindrical vessel for varying the sample-to-detector distance. The sample film was contained within a temperature-

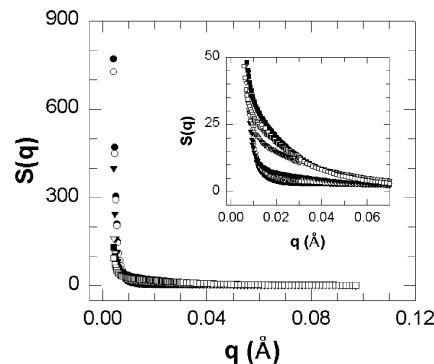


**Figure 2.** SANS data for 20% LiSdPS/mPA 50/50 blend at various temperatures: (●) 25, (○) 100, (▼) 135, (▽) 155, (■) 170, and (□) 185 °C. The inset shows the scattering at low  $q$ .

controlled sample holder made of copper. The maximum temperature possible by this setup was 200 °C. The scattering data were corrected for transmission, detector inhomogeneity, fast neutrons, and incoherent scattering. The data were radially averaged, and the intensity was rescaled to an absolute intensity using a polystyrene standard.

### Results and Discussion

**SANS.** The scattering curves for a 50/50 (w/w) 20% LiSdPS/mPA blend at various temperatures between 25 and 185 °C are shown in Figure 2. According to Figure 1, the cloud point for this blend was in excess of 250 °C, so that all of the measurements in Figure 2 were obtained well within the one-phase region. (Note that the  $M_w$  and the polydispersity of the PS used to construct Figure 1 were greater than those for the dPS used for the SANS experiments, so the cloud point curves in Figure 1 are expected to be at lower temperature than for the blends used in the present study.) For each set of data, the intensity decreased monotonically with increasing scattering vector,  $q$  (where  $q = (4\pi/\lambda) \sin(\theta/2)$  and  $\theta$  was one-half the scattering angle), which is consistent with a single phase material. The high intensity at low  $q$  for these blends indicates large long-range concentration fluctuations, which is not unexpected since blends of mPA and polystyrene are highly immiscible.<sup>21</sup> For the 50/50 blends, the scattered intensity at low  $q$  increased with increasing temperature (see inset in Figure 2), which may be due to the growth of the concentration fluctuations at elevated temperatures, even though the temperatures were still far below the phase boundary. The scattering curves for 20% LiSdPS/mPA blends with other compositions were similar to those shown in Figure 2, except that in some cases the scattering at low  $q$  decreased with increasing temperature. Those conflicting temperature dependencies may be indicative of difficulties in achieving equilibrium in these materials. While it is expected that concentration fluctuations, which are affected by the concentration and distribution of the ion-dipole complexes formed, will grow as the temperature increases toward the phase boundary, it is also recognized that complexation produces a high-viscosity solution or melt. The high viscosity affects the kinetics of complex formation during sample preparation. It is conceivable that if the sample were not originally at equilibrium, the increased chain mobility at high temperature, which normally should increase concentration fluctuations, may actually promote additional interchain complexation that suppresses concentration fluctuations.

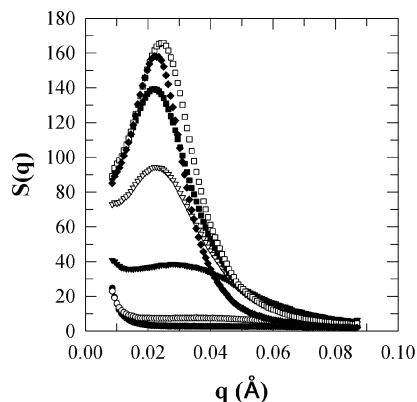


**Figure 3.** SANS scattering curves for 5.7Li-SPS/mPA blends at 100 °C: (●) 90/10, (○) 80/20, (▼) 70/30, (▽) 60/40, (■) 50/50, (□) 40/60, (◆) 20/80 SPS/mPA.

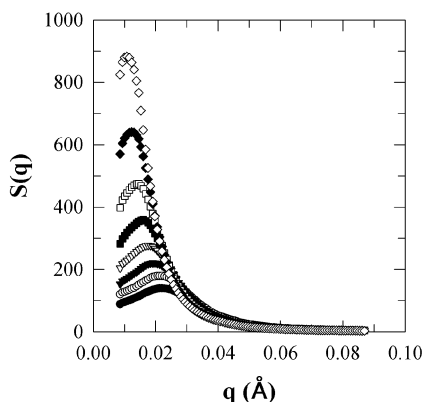


**Figure 4.** SANS scattering curves for (50/50) 5.7Li-SPS/mPA blend at (●) 100, (○) 125, (▼) 135, (▽) 145, (■) 155, (□) 165, (◆) 175, and (◇) 185 °C.

For lower sulfonation levels, the scattering curves of the blends were similar to those of the 20% LiSdPS/mPA when the ionomer concentration was high, but at higher mPA concentrations a peak was evident in the scattering patterns; Figure 3 shows the scattering of 5.7% Li-SdPS/mPA blends at 100 °C as a function of blend composition. The peak corresponded to a size in real space of  $D \sim 200\text{--}300 \text{ \AA}$ , where  $D = 2\pi/q^*$  is the Bragg spacing associated with the scattering peak and  $q^*$  is the scattering vector of the peak maximum. The peak sharpened with increasing mPA concentration and shifted to lower  $q$  (i.e., larger  $D$ ) as the temperature increased (Figure 4). A similar scattering peak was observed in the SANS data for the 8.7% LiSdPS and 11.3% LiSdPS blends.

The observation of the SANS peak was surprising because the previous light scattering experiments<sup>22</sup> indicated that the LiSdPS/mPA blends were miscible. The scattering peak indicates either a microphase-separated structure or phase inhomogeneity that was not anticipated prior to the SANS measurements. The intensity of inhomogeneity became more apparent with increasing mPA composition, and its size grew with increasing temperature. These observations are consistent with the NMR results of Gao et al.<sup>18</sup> for LiSPS/nylon-6 blends. They reported that for 70:30 (w/w) LiSPS/nylon-6 blends only a single phase was observed for a size scale  $> \sim 20 \text{ \AA}$ . However, inhomogeneities of  $\sim 50\text{--}200 \text{ \AA}$  were observed in blends with higher nylon-6 concentration. The size of the inhomogeneities detected by NMR was also sensitive to the sulfonation level for

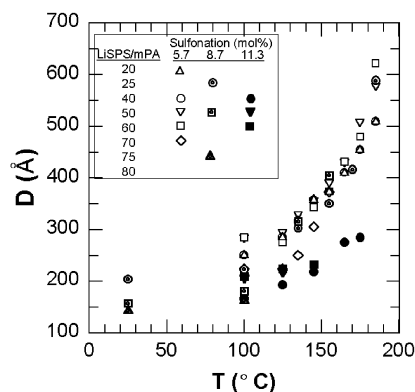


**Figure 5.** Bragg spacing associated with the SANS peak as a function of temperature, blend composition, and sulfonation level of the ionomer for LiSdPS/mPA blends.

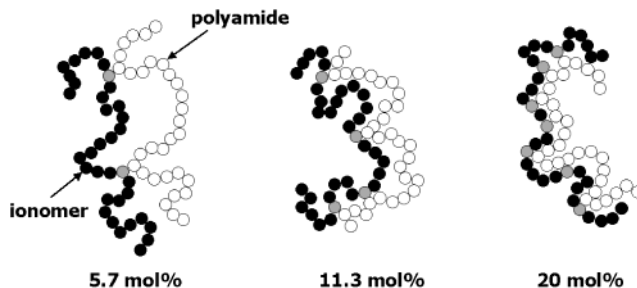


**Figure 6.** Schematic of the effect of sulfonation level of the ionomer on the suppression of concentration fluctuations between complexation points. The gray circles represent the sulfonated repeat units of the ionomer.

the ionomer; the size increased from  $\sim 20\text{--}100$  to  $\sim 50\text{--}200 \text{ \AA}$  as the polystyrene sulfonation level decreased from 9.7 to 5.4 mol %.

In general, the characteristic size of the inhomogeneity,  $D$ , increased with decreasing sulfonation level and increasing temperature (Figure 5).  $D$  also varied with blend composition, but that effect appeared to be relatively weak compared with the effects of sulfonation level and temperature, and the effect of composition was not consistent for all the different blends. That latter observation may be due in part to differences in microstructure that arose from differences in sample preparation and nonequilibrium effects.

For the LiSdPS/mPA blends, miscibility is due to strong specific complex formation between the sulfonate and amide groups.<sup>20</sup> However, polystyrene and the mPA are completely immiscible,<sup>21</sup> and accordingly, one might reasonably expect large-scale concentration fluctuations in the blend. That presumably is the origin of the high scattering intensity at very low  $q$ . The scattering peak may be a result of microphase separation or concentration fluctuations that are correlated with a characteristic separation of the complexation points, which decreases as the sulfonation level increases. Whereas light scattering experiments indicated that the blends were miscible, i.e., exhibited a single phase, those experiments probed size scales on the order of micrometers, while SANS probes size scales on the order of nanometers.

Complex formation should suppress the concentration fluctuations between the complexation points. The cartoon shown in Figure 6 shows how the characteristic sizes of concentration fluctuations between junction points are increasingly suppressed as the sulfonation level increases. As previously shown in Figure 2, at a



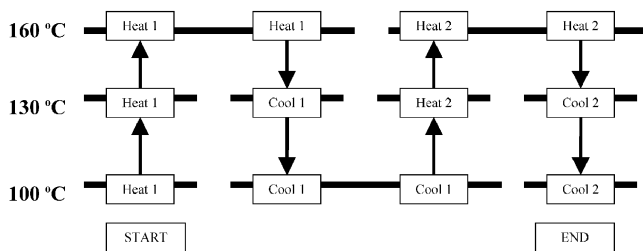


**Figure 7.** Heating and cooling scheme for assessing thermal reversibility of the blend microstructure as determined by SANS measurements. The sample was first equilibrated, and SANS measurements were made at 100 °C. The sample was then heated, and measurements were made at 130 and 160 °C. Then the sample was cooled back to 130 °C and then 100 °C, with the SANS measurements repeated at each of those temperatures. That protocol was then followed by reheating and recooling the sample, so that four replicate SANS measurements were made at 130 °C, three replicates were obtained at 100 °C, and two replicate measurements were made at 160 °C during the heating/cooling history.

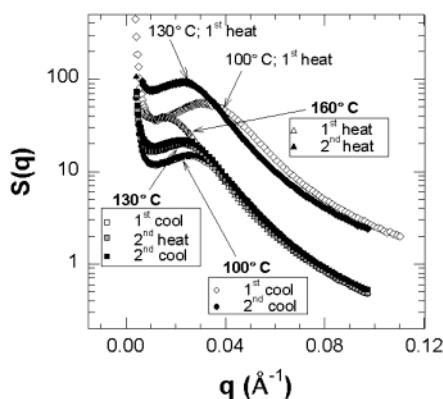


**Figure 8.** Small-angle neutron scattering data for a (50/50) 8.7LiSdPS/mPA blend as a function of thermal history, following the measurement protocol described in Figure 7.

sulfonation level of 20 mol %, no peak was observed in the SANS data of the blends, which would correspond to complete suppression of the concentration fluctuations between the complexation points, though the low- $q$  intensity upturn seen in the SANS in Figure 2 does indicate that large concentration fluctuations persisted in that system. A similar result was reported by Zhou et al.<sup>1,2</sup> for blends exhibiting intermolecular hydrogen bonding.

The reproducibility and stability of the microdomain structure were investigated by performing consecutive heating and cooling runs on a 8.7% LiSdPS/mPA 50/50 blend below the cloud point temperature. For those experiments, films cast from solution were used directly, without a subsequent thermal annealing step. Those films underwent two heating and cooling cycles from 100 to 160 °C using discrete 30 °C steps, and isothermal SANS measurements were made at 100, 130, and 160 °C during each cycle.

A schematic diagram of the heating/cooling protocol is shown in Figure 7, and the SANS data are given in Figure 8. Except for the data obtained at 100 and 130 °C during the first heating cycle, the SANS curves at any fixed temperature superposed for the various heating and cooling cycles. That result indicates that the isothermal data represent equilibrium of a thermally reversible microstructure. However, the deviation of the data for 100 and 130 °C during the first heating cycle also indicates that the sample preparation did not

produce an equilibrium state but that heating to and annealing at 160 °C were sufficient for achieving the equilibrium microstructure. Once the equilibrium microstructure was achieved, i.e., after the first heating to 160 °C, the intensity of the scattering increased as the temperature increased from 100 to 160 °C and the scattering peak moved to lower  $q$  with increasing temperature. The shift of the peak to lower  $q$  corresponds to an increase in the characteristic length associated with the peak in accordance with Bragg's law ( $D = 2\pi/q^*$ ). For these blends, the temperatures used in this experiment were well within the one-phase region determined by light scattering experiments (see Figure 1). If the origin of the peak is concentration fluctuations, these results indicate the size and intensity of the concentration fluctuations increase as temperature increases. Alternatively, if the peak represents a microphase, the size and volume fraction of that microphase increase with increasing temperature.

**Origin of the SANS Peak.** SANS data can provide information on the intermolecular interactions in a miscible blend. The most common model used to analyze SANS data for polymer blends is the random phase approximation<sup>26</sup> (RPA), which assumes mean field behavior. However, the strong ion–dipole interactions in the Li–SPS/mPA blends would appear to invalidate the RPA model for this system. In addition, the RPA model does not predict a peak in the structure factor, which also eliminates it from consideration for this particular blend system. We note, however, that in other interacting blends where a peak occurs in the SANS data the low- $q$  structure is often ignored, and the RPA is applied to the data for  $q > q^*$  (where  $q^*$  is the wavevector for which the peak in the structure factor occurs), where it is assumed that the system is randomly mixed. Because the  $q^*$  for the blends in this study were higher than what is usually observed in other blends (e.g., the hydrogen-bonded systems studied by Zhou et al. exhibited a peak in  $S(q)$  at  $q < 0.01 \text{ \AA}^{-1}$ ), we have chosen not to adopt that approach for calculating  $\chi$ .

The effect of cross-linking on the free energy of a miscible polymer blend was calculated by de Gennes<sup>27</sup> starting from classical Flory–Huggins theory for the free energy of a miscible blend. De Gennes considered a symmetric blend of polymers A and B with degree of polymerization  $N_A = N_B = N$  and volume fractions  $\phi_A = \phi_B = \phi$ , where the number of monomer units between cross-links,  $N_C$ , was much smaller than the degree of polymerization,  $N_C \ll N$ , and where the blend was randomly cross-linked with only A–B contacts. Cross-links were introduced in the homogeneous phase, after which the system was allowed to phase separate. Macroscopic phase separation was suppressed by the cross-linked structure. The structure factor of the blend is given by eq 1

$$S(q)^{-1} = \frac{C}{q^2} + \frac{1}{2}(\chi_0 - \chi) + \frac{a^2 q^2}{24} \quad (1)$$

where  $\chi$  is the interaction parameter for the cross-linked blend,  $\chi_0$  is the critical value of the interaction parameter for the un-cross-linked blend,  $a$  is the statistical segment length of the polymer chains ( $a_A = a_B = a$ ),  $q$  is the scattering vector ( $q = (4\pi/\lambda) \sin(\theta/2)$  where  $\lambda$  is the wavelength of the radiation and  $2\theta$  is the scattering angle), and  $C \approx 36/N_C^2 a^2$  is related to the “internal rigidity” of the chains.

Equation 1 predicts a maximum in the structure factor due to a "correlation hole" where microphase separation exists as a result of strong concentration fluctuations due to polymer chains that want to phase-separate but are prevented from doing so on a macroscopic scale because of the cross-links.<sup>27</sup> The length scale of the microphase separation can be approximated by the position of the scattering maximum  $q^*$ , which can be calculated from eq 1 by setting the derivative  $\partial(S(q)^{-1})/\partial q = 0$

$$q^* = \frac{5.42}{N_c^{1/2} a} \quad (2)$$

which predicts that the position of the scattering maximum,  $q^*$ , should scale with the inverse square root of the number of monomers between cross-links.

Briber and Bauer<sup>28</sup> successfully fit the de Gennes model to the SANS structure factor obtained for cross-linked blends of deuterated PS and poly(vinyl methyl ether), though the constant in eq 2 was only about one-half of that predicted by de Gennes.<sup>27</sup> The discrepancy between the experiment and theory was attributed to the fact that the internal rigidity calculation, i.e.,  $C$  in eq 1, made by de Gennes was only an approximation. The important aspect of Briber and Bauer's work was that it confirmed that eq 1 predicts the correct qualitative dependence of  $q^*$  on  $N_c$  for a cross-linked miscible blend.

The Li-SPS/mPA blends can be considered cross-linked because of the strong ion-dipole interaction that occurs between the sulfonate and amide groups. However, since the un-cross-linked blend, i.e., PS/mPA blend, is not miscible,  $\chi_0$  in eq 1 is undefined. To use the de Gennes cross-link model, we treated the term  $(\chi_0 - \chi)$  in eq 1 as a single parameter,  $\chi_{\text{eff}}$ , and assume that  $N_c$  is the average number of monomer units between sulfonate groups and  $a$  is effective bond length equal to 8 Å (allowing  $a$  to vary had little effect on the fit). Only SANS data obtained at temperatures below the cloud point as determined by light scattering were used for this analysis. Comparisons of the fit of eq 3 to experimental SANS data are shown for two different blends in Figure 9. A reasonable fit of the model was obtained for 75/25 20Li-SdPS/mPA blend, which did not exhibit a peak in the structure factor. However, in general, although the model can predict a peak in the structure factor, it did not correctly predict the position of the peak. The de Gennes cross-link model is based on four assumptions:<sup>27</sup> (i) the un-cross-linked blend is miscible; (ii) only intermolecular cross-links are formed; (iii) the blend is symmetric (i.e.,  $N_A = N_B = N$ , where  $N_i$  is the degree of polymerization of polymer  $i$ ); and (iv) the degree of polymerization between cross-link sites,  $N_c \ll N$ . The "cross-link" in these blends arises from the ion-dipole complex formed between the amide and the metal sulfonate group, which is also responsible for the miscibility of the polymers. In the absence of the sulfonate group, i.e., polystyrene, the blend is highly immiscible at all compositions, which is at odds with assumptions (i). Similarly, the cross-link is not permanent in that dissociation of the ion-dipole complex results in loss of the cross-link. In effect, the cross-link density and, therefore, the monomers between cross-link sites, is determined by a dynamic equilibrium that is affected by composition and temperature. Still, despite the noncompliance of the Li-SdPS/mPA blend

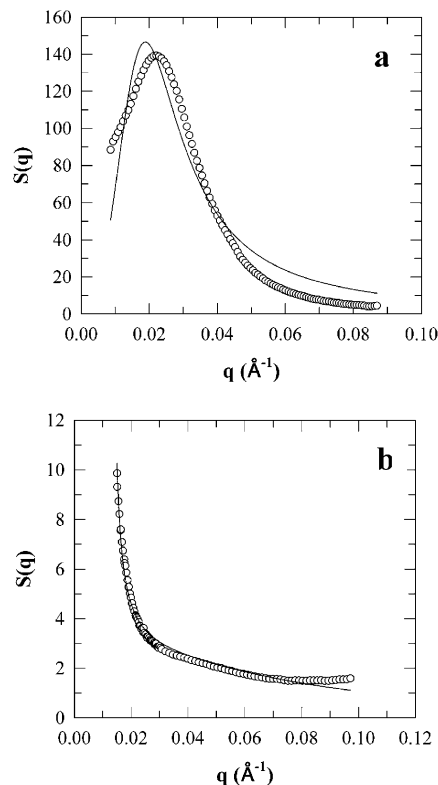


**Figure 9.** Comparison of SANS data and the de Gennes cross-link model fits for (a) the (20/80) 5.7Li-SPS/mPA blend and (b) the (75/25) 20.0Li-SPS/mPA blend. The solid lines represent the least-squares regression of the model.

system with the assumptions inherent to the de Gennes model, the model captured the qualitative features of the SANS data.

We can easily extend the de Gennes model to the case of polydisperse polymer networks. The polydispersity of the block length distribution in multicomponent block copolymers leads to an effective screening of the long-range correlations in polymer composition fluctuations.<sup>29</sup> To account for polydispersity of the network strands of the SPS/mPA melt, we added an extra parameter,  $s$ , to the last term in eq 1

$$S(x)^{-1} = x^2 + t + \left( \frac{C}{x^2 + s} \right) \quad (3)$$

where

$$x = aq \quad (4)$$

$$t = 12\chi_{\text{eff}} \quad (5)$$

The parameter  $s$  in the eq 3 is proportional to the ratio of the second and the first moments of the distribution of the number of monomers in the polymer strands between cross-links,  $s \propto \langle N_c^2 \rangle / \langle N_c \rangle$ . The "network" formed by the LiSPS/mPA complex actually has a bimodal distribution of polymer strands between cross-links, one corresponding to the distribution of the number of monomers in a polymer strand of LiSdPS and another for the mPA. Both distributions are exponential, which is a consequence of the interchain associations. For a monodisperse network, the parameter  $s$  is equal to zero and eq 3 reduces to the original de Gennes expression, eq 1.

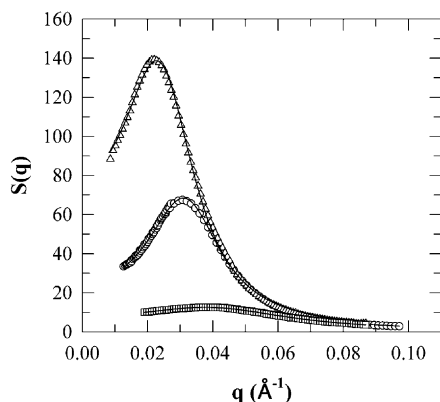


**Figure 10.** Comparison of SANS data and the modified de Gennes model fits for ( $\Delta$ ) (20/80) 5.7Li-SPS/mPA blend, ( $\circ$ ) (25/75) 8.7Li-SPS/mPA blend, and ( $\square$ ) (40/60) 11.3 Li-SPS/mPA blend. The solid lines represent the least-squares regression of the model.

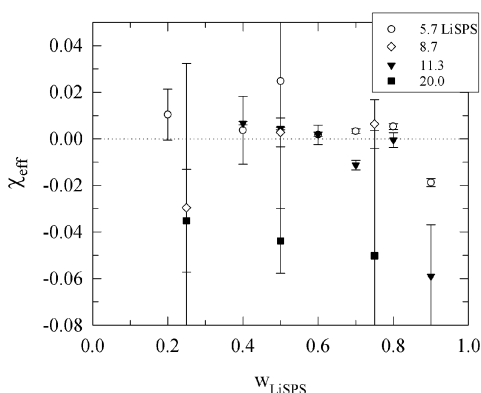


**Figure 11.** Average  $\chi_{\text{eff}}$  values calculated from the modified de Gennes model (eqs 5–9) for the Li-SdPS/mPA blends as a function of composition. The error bars represent the standard deviation (see text for explanation).

Our modified de Gennes model (MDGM), eq 3, has four adjustable parameters: the constants  $C$  and  $s$ ,  $\chi_{\text{eff}}$ , and the statistical segment length  $a$ . The MDGM did an excellent job at fitting the SANS data; three examples are shown in Figure 10. For these analyses, the statistical segment length was allowed to vary, though the values for all blends were generally about 3–5 Å at 100 °C and increased with increasing temperature. There was considerable variation in the values of  $a$ , but no obvious trend was observed with respect to sulfonation level or composition. Similarly, there was considerable variation in the values for  $C$  and  $s$ .

The effective interaction parameters,  $\chi_{\text{eff}}$ , calculated with the modified de Gennes model were relatively insensitive to temperature over the range 100–185 °C. The average values and the standard deviation are plotted for the four different sulfonation levels as a function of blend composition in Figure 11. The average and standard deviation were calculated from 5–8, 3, 7–8, and 5 temperatures for the 5.7Li-SdPS, 8.7 Li-SdPS, 11.3 Li-SdPS, and 20Li-SdPS blends, respectively. In general,  $\chi_{\text{eff}}$  decreased as the ionomer composition increased. That is expected, since there was an excess concentration of amide groups in nearly all the blends. The stoichiometry of the Li-sulfonate/carbonyl groups is plotted against composition in Figure 12. A 1:1 stoichiometry is achieved only at ionomer mass fractions of 0.94, 0.92, 0.90, and 0.84 for blends based on ionomers with sulfonation levels of 5.7, 8.7, 11.3, and

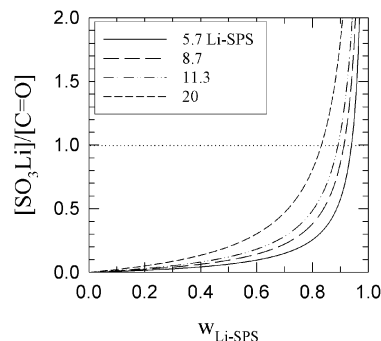


**Figure 12.** Ratio of sulfonate to carbonyl groups for LiSPS/mPA blends as a function of composition and the sulfonation level of the ionomer.

20 mol %, respectively. Except for the 90/10 11.3 Li-SdPS/mPA blend, all the blend compositions shown in Figure 10 had sulfonate/amide ratios less than 1. Therefore, as the ionomer concentration of the blend increased, more cross-links, i.e., the ion-dipole complexes, were possible. That promotes interaction of the two polymers, which is manifest by a lower  $\chi_{\text{eff}}$ .

## Conclusion

The lithium salt of sulfonated polystyrene ionomers (LiSPS) and a poly(*N,N*-dimethylethylene sebacamide) (mPA) form partially miscible blends that exhibit lower critical temperature phase (LCST) behavior.<sup>22</sup> Miscibility is the result of very strong intermolecular ion-dipole interactions that occur between the metal sulfonate and the amide carbonyl.<sup>20</sup> A peak was observed in the small-angle neutron scattering structure factor within the single-phase region for blends prepared with ionomers containing less than 20 mol % sulfonate groups. The origin of the peak is a correlation hole that arises from the formation of a pseudo-graft or cross-linked structure comprised of the two dissimilar polymer chains. Large-scale concentration fluctuations result from the inherent immiscibility of polystyrene, i.e., the polymer segments between the sulfonated styrene species, and the polyamide. The size and intensity of the concentration fluctuations increased with increasing temperature, i.e., as the LCST is approached, and decreasing sulfonation of the ionomer. Increasing the sulfonation level of the ionomer promotes more intermolecular complex formation, which suppress the concentration fluctuations. Increasing the mPA composition of the blend sharpened the scattering peak and also increased its intensity.

Because of the strong specific interactions in these blends, the scattering data cannot be treated by a mean-field approach, such as the random phase approximation.<sup>26</sup> An alternative theory, one derived for cross-linked miscible polymer blends,<sup>27</sup> does a reasonable job at predicting the qualitative features of the SANS but does not correctly predict the position of the scattering peak or the magnitude of the high- $q$  scattering. That is due, in part, to the assumption of a monodisperse network. A variation of that model, wherein polydispersity of the network was considered, quantitatively fit the SANS data for all the blends. Those model fits produced an interaction parameter,  $\chi$ , for the blends. In general,  $\chi$  decreased with increasing sulfonation level and increasing ionomer composition of the blend. Both those factors increased the number of sulfonate-amide complexes that were possible in the blend.

**Acknowledgment.** This work was supported by the Polymer Division of the National Science Foundation (Grant DMR 9712194). We also thank Mr. Jinchuan Yang and Dr. Jimmy Mays at the University of Alabama, Birmingham, and Prof. Rob Storey at the University of Southern Mississippi for the synthesis of the d-PS.

## References and Notes

- (1) Zhou, C.; Hobbie, E. K.; Bauer, B. J.; Han, C. C. *J. Polym. Sci., Polym. Phys. Ed.* **1998**, *36*, 2745.
- (2) Zhou, C.; Hobbie, E. K.; Bauer, B. J.; Sung, L.; Jiang, M.; Han, C. C. *Macromolecules* **1998**, *31*, 1937.
- (3) Coleman, M. M.; Graf, J. F.; Painter, P. C. *Specific Interactions and the Miscibility of Polymer Blends*; Technomic Publishing: Lancaster, PA, 1991.
- (4) Pearce, E. M.; Kwei, T. K.; Min, B. Y. *J. Macromol. Sci., Chem.* **1984**, *A21*, 1181.
- (5) Ziska, J. J.; Barlow, J. W.; Paul, D. R. *Polymer* **1981**, *22*, 918.
- (6) Eisenberg, A.; Hara, M. *Polym. Eng. Sci.* **1984**, *24*, 1306.
- (7) Zhou, Z. L.; Eisenberg, A. *J. Polym. Sci., Polym. Phys. Ed.* **1983**, *21*, 223.
- (8) Sen, A.; Weiss, R. A.; Garton, A. In *Multiphase Polymers: Blends and Ionomers*; Utracki, L. A., Weiss, R. A., Eds.; American Chemical Society: Washington, DC, 1989; p 353.
- (9) Lu, X.; Weiss, R. A. *Macromolecules* **1991**, *24*, 4381.
- (10) Lu, X.; Weiss, R. A. *Macromolecules* **1992**, *25*, 6185.
- (11) Kwei, T. K.; Dai, Y. K.; Lu, X.; Weiss, R. A. *Macromolecules* **1993**, *26*, 6583.
- (12) Weiss, R. A.; Lu, X. *Polymer* **1994**, *35*, 1963.
- (13) Sullivan, M. J.; Weiss, R. A. *Polym. Eng. Sci.* **1992**, *32*, 517.
- (14) Molnar, A.; Eisenberg, A. *Polymer* **1991**, *32*, 370.
- (15) Molnar, A.; Eisenberg, A. *Macromolecules* **1992**, *25*, 5774.
- (16) Molnar, A.; Eisenberg, A. *Polym. Eng. Sci.* **1992**, *32*, 1665.
- (17) Molnar, A.; Eisenberg, A. *Polymer* **1993**, *34*, 1918.
- (18) Gao, Z.; Molnar, A.; Morin, F. G.; Eisenberg, A. *Macromolecules* **1992**, *25*, 6460.
- (19) Rajagopalan, P.; Kim, J.-S.; Brack, H. P.; Lu, X.; Eisenberg, A.; Weiss, R. A.; Risen, W. M. *J. Polym. Sci., Polym. Phys. Ed.* **1995**, *33*, 495.
- (20) Feng, Y.; Schmidt, A.; Weiss, R. A. *Macromolecules* **1996**, *29*, 3909.
- (21) Feng, Y.; Weiss, R. A.; Karim, A.; Han, C. C.; Ankner, J.; Kaiser, H.; Peiffer, D. G. *Macromolecules* **1996**, *29*, 3918.
- (22) Feng, Y.; Weiss, R. A.; Han, C. C. *Macromolecules* **1996**, *29*, 3925.
- (23) Makowski, H. S.; Lundberg, R. D.; Singhal, G. H. United States 3,870,841, 1975.
- (24) Huang, S. J.; Kozakiewicz, J. *J. Macromol. Sci., Chem.* **1981**, *A15*, 821.
- (25) Han, C. C.; Bauer, B. J.; Clark, J. C.; Muroga, Y.; Masuschita, Y.; Okada, M.; Tran-cong, Q.; Chang, T.; Sanchez, I. C. *Polymer* **1988**, *29*, 2002.
- (26) De Gennes, P. G. *Scaling Concepts in Polymer Physics*; Cornell University: Ithaca, NY, 1979.
- (27) De Gennes, P. G. *J. Phys., Lett.* **1979**, *40*, L-69.
- (28) Briber, R. M.; Bauer, B. J. *Macromolecules* **1988**, *21*, 3296.
- (29) Dobrynin, A. V.; Leibler, L. *Macromolecules* **1997**, *30*, 456.

MA0341972